

SLAC-PUB-5019
SCIPP 88/32
August 1989
(T/E)

Future Limits on the ν_τ Mass^{*}

J. J. GOMEZ-CADENAS and A. SEIDEN[‡]

*Santa Cruz Institute for Particle Physics
University of California, Santa Cruz, CA 95064, USA*

and

M. C. GONZALEZ-GARCIA

Dpto. de Fisica Teorica, Valencia, Spain

and

D. COWARD and R. SCHINDLER

*Stanford Linear Accelerator Center
Stanford University, Stanford, CA 94309, USA*

Submitted to *Physical Review D*.

^{*} Work supported by Department of Energy contract DE-AC03-76SF00515.

[‡] Fulbright Fellow on leave of absence from Instituto de Fisica Corpuscular, Valencia, Spain.

ABSTRACT

In this paper, we show that the current limit on the tau neutrino mass can be improved by more than one order-of-magnitude in an experiment running at a new type of low-energy, high-luminosity collider recently proposed, the so-called Tau-Charm Factory. The design of the machine allows a luminosity of $10^{33} \text{ cm}^{-2} \text{ s}^{-1}$, at a center-of-mass energy in the range 3–4.2 GeV, thus, allowing high-precision, high-statistics studies of the τ lepton with typical production rates of the order of 10^7 τ -pairs per year.

One of the main goals of this factory would be the improvement of the current limits on the τ neutrino mass $m_{\nu\tau}$. The most promising techniques to do so is the study of the behavior of the hadronic mass spectrum in the decay $\tau^- \rightarrow \pi^- \pi^+ \pi^- \pi^+ \pi^- \nu_\tau$. To achieve a good upper limit on $m_{\nu\tau}$ from this decay, one needs not only a very high luminosity, but also an excellent detector, providing good particle identification and momentum resolution. In this paper, we attempt to quantify these detector requirements as well as to estimate the limit that can be achieved on $m_{\nu\tau}$. We show that the ν_τ mass limit can be reduced to about 3.5 to 5 MeV by this experiment.

I. INTRODUCTION

During the last few years, the issue of the ν mass has become one of the most interesting topics in particle physics and cosmology. There is no fundamental principle requiring a null mass for the neutrino. On the contrary, many extensions of the Standard Model predict nonvanishing neutrino masses *and* a mass hierarchy among different neutrino generations,¹ as is the case in the charged lepton sector. In this case, the ν_τ is predicted to be the most massive and can be the most sensitive to a mass measurement. Also, massive neutrinos could help in solving some intriguing astrophysical observations² such as the “dark matter” and “solar neutrino” problems.

While both the ν_e and ν_μ have been detected directly (that is, interactions produced by ν_e and ν_μ have been observed), the only information that we have about the ν_τ comes from the study of τ decays. Furthermore, dedicated experiments have been devoted to studying the ν_e and ν_μ masses. These experiments give a very good limit on the ν_e mass,³ $m_{\nu_e} < 18$ eV, and a fairly good limit on the ν_μ mass,⁴ $m_{\nu_\mu} < 250$ keV. In contrast, the τ neutrino mass has only been studied in general purpose e^+e^- experiments. The current best upper limit on m_{ν_τ} is much higher than the ones on the electron and muon neutrino masses,⁵ $m_{\nu_\tau} < 35$ MeV. This limit could be very much improved by an experiment running at a new type of e^+e^- collider. It has recently been proposed^{6,7} to build a new low-energy, high-luminosity machine, the so-called Tau-Charm Factory. The design luminosity for this machine is 10^{33} cm⁻² s⁻¹, with a center-of-mass energy range of about 3–4.2 GeV. At this luminosity, typical rates of 10^7 τ -pairs per year could be produced. This is illustrated in Fig. 1, where we show the τ velocity β

and the τ -pair production cross section, as a function of the center-of-mass energy. For this paper, we will assume that a year of data-taking corresponds to 5000 hours ($1.8 \cdot 10^7$ seconds); then, the number of τ -pairs produced per year for the design luminosity of $10^{33} \text{ cm}^{-2} \text{ s}^{-1}$ is obtained directly from Fig. 1(b) by simply multiplying the value corresponding to the cross section in nb by $1.8 \cdot 10^7$.

In principle, the two most promising experimental techniques to set a limit on $m_{\nu\tau}$ are the study of the spectrum of the lepton (electron or muon) in the decay $\tau \rightarrow l\bar{\nu}_l\nu_\tau$, and the study of the end point of the hadronic mass spectrum of high multiplicity τ decays. In particular the decay $\tau^- \rightarrow \pi^-\pi^+\pi^-\pi^+\pi^-\nu_\tau$ has been used to set the best current limit on $m_{\nu\tau}$.^{a)}

It has been shown^{8,9} that the best limit on $m_{\nu\tau}$ that can be achieved in a Tau-Charm Factory by studying the decay $\tau \rightarrow l\bar{\nu}_l\nu_\tau$, is of the order of 20–30 MeV, thus providing little improvement on the current limit. In this paper, we show that the limit on $m_{\nu\tau}$ that can be obtained from the decay $\tau^- \rightarrow \pi^-\pi^+\pi^-\pi^+\pi^-\nu_\tau$ is one order-of-magnitude better. We study the most important problems, such as event selection, background suppression, and detector requirements to achieve a $m_{\nu\tau}$ limit of 3.5 to 5 MeV at 90% CL. In Sec. II, we discuss the general characteristics of the decay $\tau^- \rightarrow \pi^-\pi^+\pi^-\pi^+\pi^-\nu_\tau$ and the model that we have used to simulate it. In Sec. III, we describe our projected detector. In Sec. IV, we discuss the event selection and background suppression; while in Sec. V, we obtain the limits that can be achieved on $m_{\nu\tau}$. Finally, in Sec. VI, we present our conclusions.

a) References in this paper to a specific charge state are to be interpreted as also implying to the charge conjugate state.

II. THE DECAY $\tau^- \rightarrow \pi^- \pi^+ \pi^- \pi^+ \pi^- \nu_\tau$

The hadronic decays of the τ are due to the coupling of the charged weak current to hadrons, which in the case of the decay $\tau^- \rightarrow \pi^- \pi^+ \pi^- \pi^+ \pi^- \nu_\tau$ reduces to the coupling of the W boson to the ud current. The decay amplitude can be written as

$$M = \frac{G_F^2}{\sqrt{2}} \cos \theta_c \bar{u}_{\nu_\tau} \gamma^\mu (1 - \gamma_5) u_\tau H_\mu \quad , \quad (1)$$

with u_τ and u_{ν_τ} being the spinors of the τ and the ν_τ , respectively; θ_c , the Cabibbo angle, and

$$H_\mu = \langle 0 | \bar{v}_d \gamma^\mu (1 - \gamma_5) u_u | 5\pi \rangle \quad ,$$

the hadronic current. Squaring and averaging over the τ polarizations, we obtain

$$|\bar{M}|^2 = 2G_F^2 \cos^2 \theta_c [2(p'^\mu p^\nu) - (pp')g^{\mu\nu}] H^\mu H^{\nu*} \quad , \quad (2)$$

where p^μ and p'^μ are the τ and ν_τ momenta. We can now write

$$d\Gamma(\tau^- \rightarrow \pi^- \pi^+ \pi^- \pi^+ \pi^- \nu_\tau) = \frac{1}{2m_\tau} |\bar{M}|^2 d\Phi_6 \quad , \quad (3)$$

where $d\Phi_6$ is the six-body phase-space volume. Integration over the five-pion phase space yields

$$d\Gamma = \frac{G_F^2 \cos^2 \theta_c}{m_\tau (2\pi)^3} [2(p'^\mu p^\nu) - (pp')g^{\mu\nu}] \frac{d^3 p'}{2E'} \int d\Phi_5 H^\mu H^{\nu*} \quad . \quad (4)$$

In the approximation of a conserved axial current, we can write

$$\int d\Phi_5 H^\mu H^{\nu*} = 2\pi (q^\mu q^\nu - g^{\mu\nu} q^2) h(q^2) \quad ; \quad (5)$$

here, $q^\mu = p^\mu - p'^\mu$ is the momentum transfer, and therefore q^2 is the squared

invariant mass of the system. Integrating over the ν_τ solid angle, we write in terms of q^2 ,

$$d\Gamma = \frac{G_F^2 \cos^2 \theta_c}{m_\tau^2 4\pi} [2(p'q) - (p'q) + (pp')q^2] |\mathbf{p}'| h(q^2) dq^2 \quad . \quad (6)$$

Finally, taking into account momentum conservation, $q^\mu = p^\mu - p'^\mu$, we obtain

$$d\Gamma = \frac{G_F^2 \cos^2 \theta_c}{m_\tau^2 8\pi} \varpi(q^2, m_\tau^2, m_{\nu_\tau}^2) \lambda^{1/2}(m_\tau^2, q^2, m_{\nu_\tau}^2) h(q^2) \quad , \quad (7)$$

where $\varpi(q^2, m_\tau^2, m_{\nu_\tau}^2)$ is the so-called weak matrix element,

$$\varpi(q^2, m_\tau^2, m_{\nu_\tau}^2) = (m_\tau^2 - q^2)(m_\tau^2 + 2q^2) - m_{\nu_\tau}^2(2m_\tau^2 - q^2 - m_{\nu_\tau}^2) \quad ,$$

and

$$\lambda^{1/2}(m_\tau^2, q^2, m_{\nu_\tau}^2) = \{[m_\tau^2 - (\sqrt{q^2} + m_{\nu_\tau})^2][m_\tau^2 - (\sqrt{q^2} - m_{\nu_\tau})^2]\}^{1/2} = 2m_\tau |\mathbf{p}'| \quad .$$

The function $h(q^2)$ factorizes our ignorance about the hadronic structure of the decay $\tau^- \rightarrow \pi^- \pi^+ \pi^- \pi^+ \pi^- \nu_\tau$. With the currently available experimental data, very little is known about the possible resonance structure mediating it, and thus, about the form of $h(q^2)$. In spite of that, we know that due to the limited phase space, the neutrino emitted in the decay $\tau^- \rightarrow \pi^- \pi^+ \pi^- \pi^+ \pi^- \nu_\tau$ typically has low momentum (since the hadronic system tends to have a large invariant mass) and therefore, the end point of the hadronic mass spectrum is very sensitive to the τ neutrino mass. At the end point of the spectrum, we have simply:

$$m_{\nu_\tau} = m_\tau - m_{had} \quad ,$$

where $m_{had} = \sqrt{q^2}$ is the hadronic mass of the five pions. To determine m_{ν_τ} , it is necessary to compare the hadronic mass distribution with the functional form

expected from the theory with the ν_τ mass as an adjustable parameter. This function is obtained from Eq. (7) as:

$$\frac{d\Gamma}{dm_{had}} \propto m_{had} \varpi(q^2, m_\tau^2, m_{\nu_\tau}^2) \lambda^{1/2}(m_\tau^2, q^2, m_{\nu_\tau}^2) h(q^2) . \quad (8)$$

As we have mentioned above, the exact form of $h(q^2)$ is not predicted in the case of the decay $\tau^- \rightarrow \pi^- \pi^+ \pi^- \pi^+ \pi^- \nu_\tau$, and thus the exact shape of the hadronic mass distribution is not known. However, the theoretical study of another high-invariant mass τ decay ($\tau^- \rightarrow K^- K^+ \pi^- \nu_\tau$) for which a suitable model exists,^{10,11} provides us with some clues relative to the expected behavior of the invariant mass distribution for the decay $\tau^- \rightarrow \pi^- \pi^+ \pi^- \pi^+ \pi^- \nu_\tau$:

- (i) The shape of the distribution at the end point depends only very weakly on the actual resonance structure.
- (ii) The population close to the end point of the invariant mass distribution will, however, depend dramatically on this structure.

To quantify these two points, we have Monte-Carlo generated the decay $\tau^- \rightarrow \pi^- \pi^+ \pi^- \pi^+ \pi^- \nu_\tau$ through simple five-pions phase space for the $h(q^2)$ function (no intermediate resonance structure) and through phase space for different possible intermediate resonance structures: $\tau^- \rightarrow A_1^-(1260) \pi^+ \pi^- \nu_\tau$ (with the A_1 then decaying to three charged pions); $\tau^- \rightarrow \rho^-(770) \pi^- \pi^+ \pi^- \nu_\tau$ and $\tau^- \rightarrow \rho^-(770) \rho^+(770) \pi^- \nu_\tau$, where the ρ subsequently decays into two charged pions. In Figs. 2 and 3, we show the hadronic mass distributions in the allowed range of values [Figs. 2(a) and (b)] and close to the end point of the distribution $m_{had} > 1.75$ GeV [Figs. 3(a) and (b)] for the pure phase-space model, and the $\tau^- \rightarrow$

$\rho^0 \rho^0 \pi^- \nu_\tau$ model. Notice that the shapes of the invariant mass distributions are identical when close to the end point, even when the final pions are produced in the second case via a complicated system of resonances. This is due to the fact that the end point of the invariant mass distribution in the decay $\tau^- \rightarrow \pi^- \pi^+ \pi^- \pi^+ \pi^- \nu_\tau$ is completely dominated by the weak matrix element and the kinematical function $\lambda^{1/2}(m_\tau^2, q^2, m_{\nu_\tau}^2)$. Nevertheless, since the distribution for the τ decay with no intermediate resonance structure peaks at lower masses than the distribution for the decay $\tau^- \rightarrow \rho^0 \rho^0 \pi^- \nu_\tau$, the end point of the invariant mass distribution has a much smaller population in the first case than in the second.

On the other hand, the currently available experimental data for the decay $\tau^- \rightarrow \pi^- \pi^+ \pi^- \pi^+ \pi^- \nu_\tau$ from the Argus experiment⁵ suggests that it must be dominated by some resonance structure that makes the distribution peak to large invariant masses. Little can be said about this structure, since there are several combinations of known resonances that can produce five charged pions on the final state, and it could be additional, yet unknown resonances. Moreover, we do not have any model that describes the dynamics of the possible combination of intermediate states. However, for our study we have assumed the model in which the τ decays to five charged pions via the intermediate channel $\tau^- \rightarrow \rho^0 \rho^0 \pi^- \nu_\tau$. Although an obvious simplification of the real structure, this model presents two nice features: it decays 100% of the time to five charged pions *and* give us a mass distribution in good agreement with the experimental data (see Fig. 2). Furthermore, as we have discussed above, the details of the resonance structure will be washed out close to the end point of the invariant mass distribution, and therefore, the limits on m_{ν_τ} will not depend strongly on the model used except for the statistics

that can be achieved near the end point.

From the discussion above, it is clear that the limits that we can project for $m_{\nu\tau}$ depend on our knowledge (or rather, lack of it) on the $\tau^- \rightarrow \pi^- \pi^+ \pi^- \pi^+ \pi^- \nu_\tau$ intermediate structure. However, since our model for simulating the decay $\tau^- \rightarrow \pi^- \pi^+ \pi^- \pi^+ \pi^- \nu_\tau$ via $\tau^- \rightarrow \rho^0 \rho^0 \pi^- \nu_\tau$ agrees well with the available data, we can hope that our results will be reasonably realistic.

III. THE TAU-CHARM FACTORY EXPERIMENT FOR MEASURING $m_{\nu\tau}$

To study the limits on $m_{\nu\tau}$ that can be achieved in an experiment running at a Tau-Charm Factory, we have made a simulation of this experiment. A preliminary design of the proposed accelerator has been given in Ref. 12 and further work is discussed in Ref. 7. A detector design has also been discussed in Ref. 7. Here, we will only outline its main features. A schematic view of the detector is shown in Fig. 4. Its main components are:

- (i) A thin (0.8 mm), low- Z material (beryllium) beam pipe to minimize multiple Coulomb scattering. The beam pipe radius is optimized at 5 cm.
- (ii) A high-resolution drift chamber characterized by the following parameters:

Momentum measurement precision: $[\sigma_p/p]^2 = [0.4\%p(\text{GeV})]^2 + [0.3\%/\beta]^2$.

P_\perp^{\min} for efficient tracking: 75 MeV.

θ_{\min} for efficient tracking: $|\cos \theta| < 0.95$.

Hermetic: No cracks.

- The chamber is a cylindrical volume of radius 100 cm and length 360 cm operating in a moderate magnetic field of 0.6 T. The inner wall is contiguous with the beam pipe to allow a vertex constrained fit which will improve the measurement of the track angles. The drift chamber gas must be light, to minimize multiple scattering. This can be accomplished by using helium-rich mixtures (for the simulation of the detector, we presently use a mixture of 72% helium, 15% carbon dioxide and 7% isobutane at a pressure of 1 atm).
- (iii) A time-of-flight (TOF) system positioned at a radius of 105 cm and with a 120 ps resolution. The TOF is able to separate π from K at the 3σ level for momentum less than 1100 MeV.
- (iv) An electromagnetic calorimeter (EMC) made of 14 radiation lengths of CsI crystals covering 95% of the solid angle. The calorimeter energy resolution is assumed to be $\sigma_E/E = 2\%/\sqrt{E}$ and is able to discriminate photons with energy as low as 25 MeV.
- (v) A combined hadron calorimeter and muon detector (HDC) made of five interaction lengths of Fe with a 3 cm sampling also covering 95% of the solid angle. We assume that neutrals hadrons with energy bigger than 50 MeV can be identified by this detector.

Particle identification is achieved in the detector through the combination of electromagnetic and hadronic calorimetry, muon range and angle measurements, and TOF and dE/dx measurements. Since the average particle momentum in a Tau-Charm Factory experiment is low ($P < 1$ GeV) these techniques are very effective. Our global rejection factor to separate electrons (muons) from hadrons

using this techniques is of the order of 10^{-3} (10^{-2}).

For our study, we have developed a full simulation of the detector. For each simulated event, the particles are transported through the detector. The effect of multiple Coulomb scattering and energy loss in the beam pipe and in the chamber material is taken into account, as well as the detector inefficiencies, cracks, etc. Our τ generator incorporates different models for the decay $\tau^- \rightarrow \pi^- \pi^+ \pi^- \pi^+ \pi^- \nu_\tau$. For the simulation of the hadronic background, we have used the Lund Monte Carlo.¹³

IV. EVENT SELECTION AND BACKGROUND SUPPRESSION

In this section, we discuss our selection criteria and show that they result in a statistically significant signal with negligible background.

First, we have to decide on the optimum energy for the experiment. We have set $\sqrt{s} = 3.680$ GeV, close to the cross section peak (see Fig. 1), but still away from the $\psi(3685)$ resonance. At this energy, we have the advantage of having high τ pair rates without producing charmed mesons, which are a potentially dangerous background to our process.

At $\sqrt{s} = 3.680$ GeV, the boost of the particles emitted in τ decays is very small and thus, the decay products of one τ cannot be distinguished from those of the other looking at the event topology. Therefore, we only accept τ -pairs where one of the τ 's decays via $\tau^- \rightarrow \pi^- \pi^+ \pi^- \pi^+ \pi^- \nu_\tau$ and the other results in a clean lepton “tag,” $\tau \rightarrow e \bar{\nu}_e \nu_\tau$ or $\tau \rightarrow \mu \bar{\nu}_\mu \nu_\tau$. In order to guarantee good lepton identification, we only accept the event if the tag momentum is sufficiently high,

$P_{lepton} > 400$ MeV. Our signal is therefore characterized by several distinctive features:

- (1) High charged multiplicity (six charged tracks).
- (2) Neither electromagnetic nor hadronic neutral energy in the event, not associated with charged tracks.
- (3) One (and only one) lepton of (relatively) high momentum.
- (4) Large missing momentum recoiling versus the lepton. Since the ν_τ emitted in the decay $\tau^- \rightarrow \pi^- \pi^+ \pi^- \pi^+ \pi^- \nu_\tau$ typically has low momentum, almost all the missing momentum in the event is due to the neutrinos emitted in the decay $\tau \rightarrow l \bar{\nu}_l \nu_\tau$.

The selection criteria take advantage of these features. We impose the following requirements.

- (i) Exactly six charged tracks within the tracking detector volume. To guarantee good momentum measurement, we accept tracks only in the angular range $|\cos \theta| < 0.9$ (where θ is the polar angle to the beam) and with a minimum transverse momentum greater than 100 MeV.
- (ii) The electromagnetic energy (not associated with a charged track) deposited in the EM must be less than 30 MeV, while the hadronic neutral energy deposited in the HDC must be smaller than 50 MeV.
- (iii) One track identified as an electron (or muon) of momentum bigger than 400 MeV. The other five tracks must be identified as pions.
- (iv) The missing momentum of the event, P_{miss} , must be bigger than 400 MeV.

Also, the missing momentum vector must point into the good tracking volume of the detector, $|\cos \theta_{miss}| < 0.9$.

(v) We define the reduced mass of the event as

$$m_{reduced} = \sqrt{(E_{lepton} + E_{miss})^2 - (\mathbf{P}_{lepton} + \mathbf{P}_{miss})^2} .$$

Since almost all the missing momentum in the signal is due to the neutrinos in the decay $\tau \rightarrow l\bar{\nu}_l\nu_\tau$, the reduced mass will tend to peak at the τ mass, while in the case of background events where the lepton tag is faked by the decay in flight of a K or a π , the reduced mass will tend to peak at lower values. Therefore, we impose the reduced mass to be larger than the kaon mass.

In Fig. 5(a), we show the lepton momentum distribution, while in Fig. 5(b), we show the inclusive momentum spectrum P_{inc} of the five pions in the decay $\tau^- \rightarrow \pi^- \pi^+ \pi^- \pi^+ \pi^- \nu_\tau$ (assuming a phase-space model). The missing momentum and reduced mass distributions are shown in Fig. 6.

At $\sqrt{s} = 3.680$ GeV, we obtain $4.5 \cdot 10^7$ τ -pairs per year. Then the number of tagged events we expect per year is:

$$N_{tagged}^\tau = 9 \cdot 10^7 (B_{\tau \rightarrow e\bar{\nu}_e\nu_\tau} + B_{\tau \rightarrow \mu\bar{\nu}_\mu\nu_\tau}) B_{\tau^- \rightarrow \pi^- \pi^+ \pi^- \pi^+ \pi^- \nu_\tau} \epsilon ,$$

where ϵ is the efficiency for passing the selection criteria. Taking $B_{\tau \rightarrow e\bar{\nu}_e\nu_\tau} = B_{\tau \rightarrow \mu\bar{\nu}_\mu\nu_\tau} = 18\%$, $B_{\tau^- \rightarrow \pi^- \pi^+ \pi^- \pi^+ \pi^- \nu_\tau} = 0.06\%$,⁵ we obtain

$$N_{tagged}^\tau = 20000 \cdot \epsilon \text{ per year} .$$

The main reasons for loss of signal events are the strict requirements to track all

the six particles in the event (only 41% of the signal events pass this first cut), and the minimum momentum cut for the leptonic tag. In Table 1, we illustrate how the selection criteria reduce our signal data sample for a one year run. Our efficiency ϵ is about 30%. However, only 7% of the tracks passing the cuts are in the mass range of interest ($m_{had} > 1750$ MeV). Thus, about 2% of the tagged events make it into the final sample.

On the other hand, our selection criteria will provide a very efficient suppression of the background. The only relevant background events for our process are multihadronic events

$$e^+e^- \rightarrow \gamma \rightarrow u, d, s \rightarrow 6 \text{ charged tracks} \quad .$$

Before the cuts, the ratio R of signal to potential background is

$$R = \frac{\sigma_{\tau\tau} B_{\tau^- \rightarrow \pi^- \pi^+ \pi^- \pi^+ \pi^- \nu_\tau} 2B_{\tau^- \rightarrow l \bar{\nu}_l \nu_\tau}}{\sigma_{had} B_c} \quad .$$

Here, B_c is defined as the branching fraction of multihadronic events with six charged tracks (and any number of neutrals) in the final state, $B_c \sim 10\%$. Since $\sigma_{had}/\sigma_{\tau\tau} \sim 6.5$, we obtain $R = 5 \cdot 10^{-4}$. However, our selection criteria will provide a rejection against the background of the order of 10^7 ; thus, after the cuts, $R > 10^3$. This is due to the following reasons.

- (a) The hadronic backgrounds have high neutral multiplicity, while the signal has no neutral energy. Notice that very hermetic electromagnetic and hadronic calorimeter with minimum cracks are needed for this selection criteria to be effective.

- (b) We require exactly one high-momentum lepton. The leptons in the hadronic background are due to gamma conversions and Dalitz decays (for electrons) and decays in flight and hadron misidentification (for muons). The momentum spectrum is peaked at low energy. This is illustrated in Fig. 7, where we show the momentum distribution for the lepton (taken to be an electron) in the signal and in the hadronic background.
- (c) There are no emitted neutrinos in the hadronic background. Therefore, the missing momentum peaks close to zero. Also, the reduced mass of the hadronic background peaks at low values as discussed above. This is shown in Fig. 8(a) and (b).
- (d) Finally, the hadronic mass of the background is always very large, since at this low energy, the multihadron events tend to be very spherical. This can be seen in Fig. 9.

In Table 1, we show how our selection criteria reduce the background. We find a rejection better than 10^5 without using the reduced mass cut that will provide an additional rejection of at least a factor of 10. The fact that the hadronic mass of the background events is always very high guarantees an additional suppression of at least another order of magnitude. We have also studied other possible potential backgrounds, such as radiative Bhabha scattering and higher-order QED processes, and found them all negligible. We conclude that if the projected detector requirements are met, we can obtain an essentially background-free data sample.

V. LIMITS ON $m_{\nu\tau}$

Once the events have passed the selection criteria, we compute the invariant

mass of the hadronic system. Due to the low average momentum of the pions emitted in the decay $\tau^- \rightarrow \pi^- \pi^+ \pi^- \pi^+ \pi^- \nu_\tau$, the momentum resolution (and thus the hadronic mass resolution) is completely dominated by the multiple scattering of the pions in the chamber material. With our projected resolution ($0.3\%/\beta$ for the multiple scattering term), we obtain a mass resolution of 2 MeV. We have also investigated the effect of the multiple scattering of the pions in the beam pipe and found it to be small.

To estimate the sensitivity that can be achieved on the tau neutrino mass, we have generated decays $\tau^- \rightarrow \pi^- \pi^+ \pi^- \pi^+ \pi^- \nu_\tau$ assuming different neutrino masses ($m_{\nu_\tau} = 1, 5, 10$ and 20 MeV) and performed a χ^2 minimization fit to the corresponding distributions. We have fit the end point of the hadronic mass distribution ($m_{had} > 1.75$ GeV) to Eq. (8) folded with a resolution function describing the detector mass resolution. As discussed in Sec. II, the specific form of the function $h(m_{had}^2)$ describing the decay structure is of little relevance on the fit results, since the end point of the invariant mass distribution is completely dominated by the weak matrix element and the kinematical function $\lambda^{1/2}(m_\tau^2, q^2, m_{\nu_\tau}^2)$.

We have considered both a “one-year” (350 events in the mass range $m_{had} > 1.75$ GeV) and a “two-year” run (700 events in the same range). Within a year, we obtain a limit on m_{ν_τ} of 5.0 MeV. This limit is reduced to 3.5 MeV in another year’s run. To illustrate our technique, in Fig. 10, we show the distributions and best fits for four different ν_τ masses, corresponding to a “two-year” run period.

One obvious condition for obtaining this result is that the error on the τ mass be much smaller than the present value of 3.2 MeV. However, one of the first experiments that can be done easily in a Tau-Charm Factory will reduce the error

on the τ mass to about 250 keV. This has been discussed in Ref. 7.

VI. CONCLUSIONS

We have considered the possibility of improving the ν_τ mass limit with an experiment running at a Tau-Charm Factory by studying the hadronic mass distribution in the decay $\tau^- \rightarrow \pi^- \pi^+ \pi^- \pi^+ \pi^- \nu_\tau$. We show that with the projected luminosity and detector capabilities, this experiment may be able to improve the present limit on the τ neutrino mass up to a factor of 10. However, the “running time” that we quote depends on the model that we have used to simulate the decay $\tau^- \rightarrow \pi^- \pi^+ \pi^- \pi^+ \pi^- \nu_\tau$. Other models will modify the population of the end point of the hadronic invariant mass distribution and therefore, the time needed for the experiment. As we have discussed in Sec. II, our model well describes the available experimental data. However, other models that decrease (*i.e.*, a mixture of the $\rho\rho\pi$ and $\rho\pi\pi\pi$ resonances) or increase [*i.e.*, a mixture of $\rho\rho\pi$ and $\rho'(1600)\pi$] the population of the end point can also give results compatible with the experimental data.

To conclude, it seems certainly possible to investigate the neutrino mass to the few-MeV level using the decay $\tau^- \rightarrow \pi^- \pi^+ \pi^- \pi^+ \pi^- \nu_\tau$. Whether it will take a few months or a few years remains to be seen.

ACKNOWLEDGMENTS

We are very indebted to P. Burchat, A. Pich, and S. Weseler for many useful discussions. We also profited from discussions with C. A. Heusch, J. Kirkby, L. Labarga, W. Lockman, and M. Perl. Finally, J. J. G. wants to acknowledge the Fulbright grant which has made possible his stay at SCIPP.

REFERENCES

- ¹ For a review, see J. W. F. Valle, Theory and implications of neutrino mass. FTUV/5-89. Invited lectures given at the 10th Autumn School on Physics. Lisbon, Portugal. Submitted to Nucl. Phys.
- ² J. Silk, Proceedings of the XXIII International Conference on High Energy Physics, Berkeley, ed. C. S. Loken (World Scientific, 1986) p. 465.
- ³ M. Fritschi *et al.*, Phys. Lett. **173B** (1986) 485.
- ⁴ R. Abela, Phys. Lett. **146B** (1984) 431.
- ⁵ H. Albrecht *et al.*, Phys. Lett. **202B** (1988) 149.
- ⁶ J. Kirkby, CERN-EP/87-210, 1987.
- ⁷ See proceedings of the Tau-Charm Factory Workshop, SLAC Report-343, to be published.
- ⁸ R. R. Mendel *et al.*, Z Phys. **C32** (1986) 517.
- ⁹ J. J. Gomez-Cadenas and M. C. Gonzalez-Garcia, Phys. Rev. **D39** (1989) 1370.
- ¹⁰ M. C. Gonzalez-Garcia, J. J. Gomez-Cadenas, and A. Pich, SCIPP 26/89
- ¹¹ A. Pich *et al.*, Nucl. Phys. **321B** (1989) 311.
- ¹² J. Jowett, CERN-LEP-TH/87-56 (1987).
- ¹³ T. Sjostrand and M. Bengtsson, Comput. Phys. Commun. 43 (1987) 367.

Table 1. Events passing the selection criteria.

Events	Signal	Background
Analyzed	20000	107350
With six charged tracks (cut- <i>i</i>)	8250	21629
No neutral in event (cut- <i>ii</i>)	8010	1476
One electron vs. five pions (cut- <i>iii</i>)	6003	3
$P_{miss} > 400$ MeV (cut- <i>iv</i>)	5300	0
$m_{reduced} > m_{kaon}$ (cut- <i>v</i>)	4900	0
# of events with $1.75 < m_{had} < 1.79$ GeV	350	0

FIGURE CAPTIONS

1. (a) τ velocity β and (b) τ -pair production cross section (lowest order), as a function of the center-of-mass energy.
2. Hadronic invariant mass distributions for the decay $\tau^- \rightarrow \pi^- \pi^+ \pi^- \pi^+ \pi^- \nu_\tau$; (a) with no intermediate resonance structure (five-body phase-space), and (b) through the intermediate channel $\tau \rightarrow \rho \rho \pi \nu_\tau$: we superimpose Argus data.
3. Hadronic invariant mass distributions for the decay $\tau^- \rightarrow \pi^- \pi^+ \pi^- \pi^+ \pi^- \nu_\tau$ close to the end point ($m_{had} > 1750$ MeV): (a) five-body phase-space, (b) through the intermediate channel $\tau \rightarrow \rho \rho \pi \nu_\tau$. The normalization of both distributions is the same.
4. The Tau-Charm Factory detector.
5. (a) Lepton momentum spectrum from the decay $\tau \rightarrow l \bar{\nu}_l \nu_\tau$. (b) Inclusive 5- π spectrum in the decay $\tau^- \rightarrow \rho^0 \rho^0 \pi^- \nu_\tau \rightarrow \tau^- \rightarrow \pi^- \pi^+ \pi^- \pi^+ \pi^- \nu_\tau$.
6. (a) Missing momentum distribution for the signal. (b) Reduced mass for the signal.
7. The lepton momentum spectrum for the signal (the tag taken to be $\tau \rightarrow e \bar{\nu}_e \nu_\tau$) and the hadronic background (shaded). The arrow indicates the selection cut.
8. (a) Missing momentum for the signal and the hadronic background (shaded). (b) Reduced mass for the signal and the hadronic background (shaded). The arrow indicates the selection cut.

9. Hadronic mass for the signal and the hadronic background (shaded). The arrow indicates the selection cut.
10. The hadronic mass distributions for different neutrino masses, together with the best fit to them. The distributions correspond to the case of 700 events passing the selection criteria (two-year run).

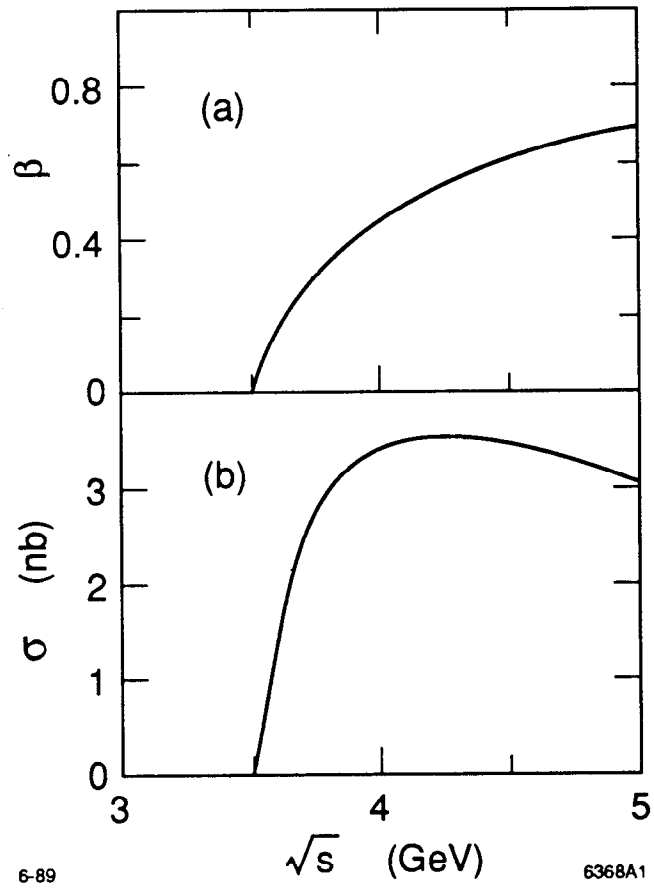


Fig. 1

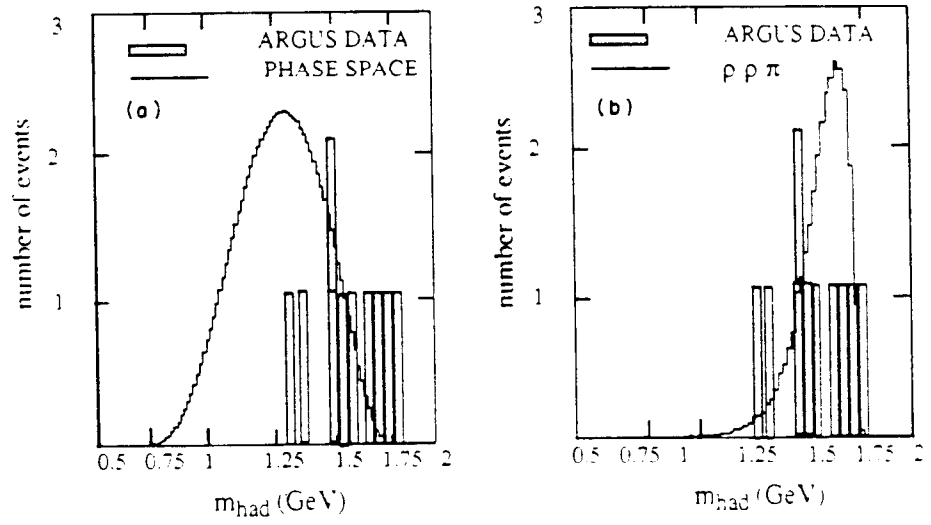


Fig. 2

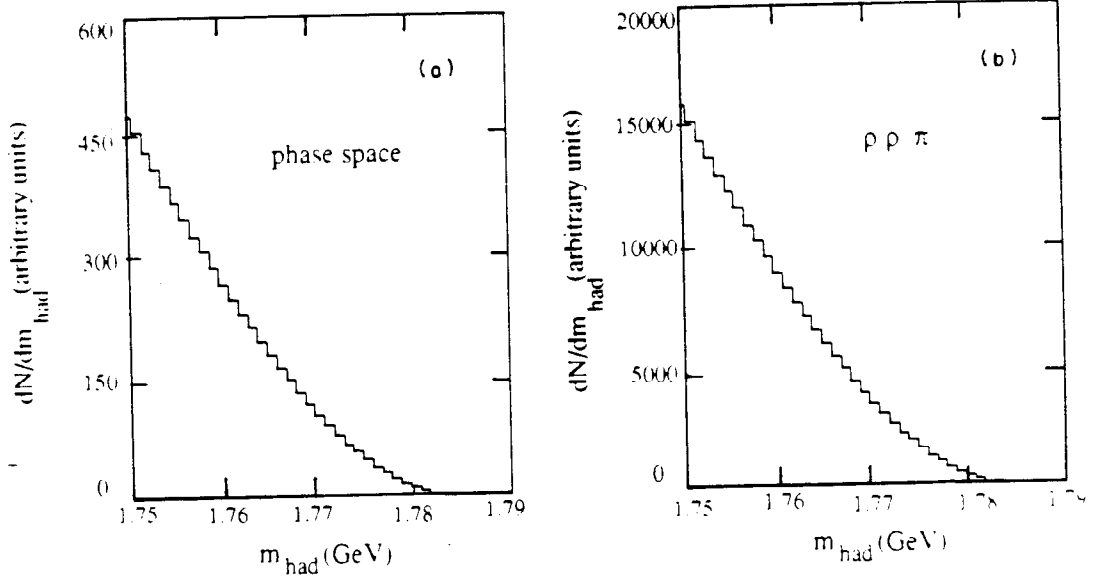


Fig. 3

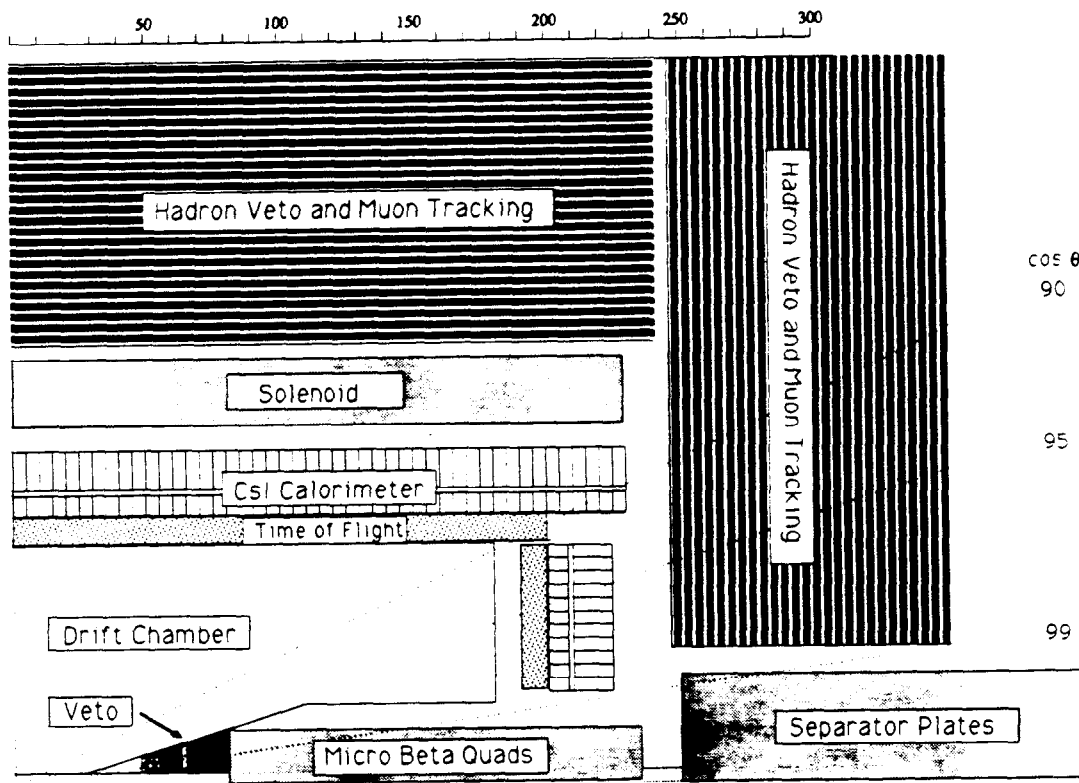
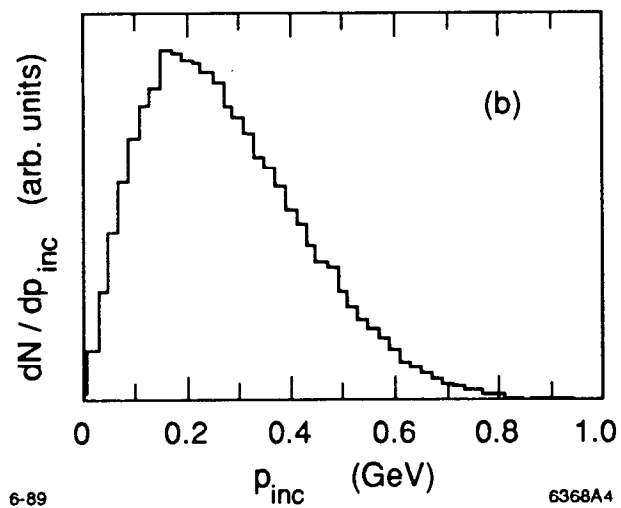
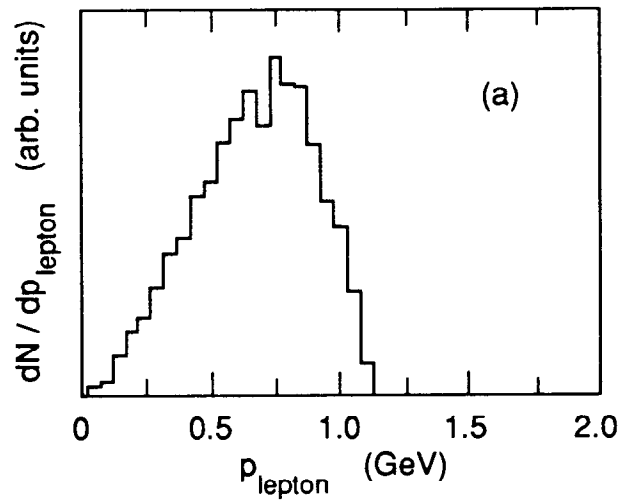


Fig. 4



6-89

6368A4

Fig. 5

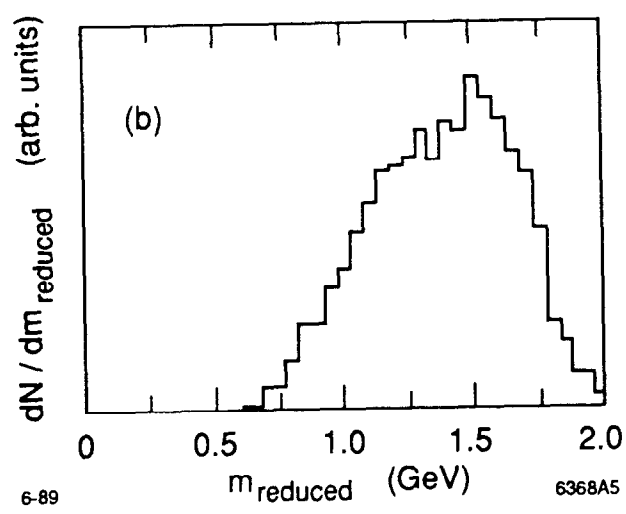
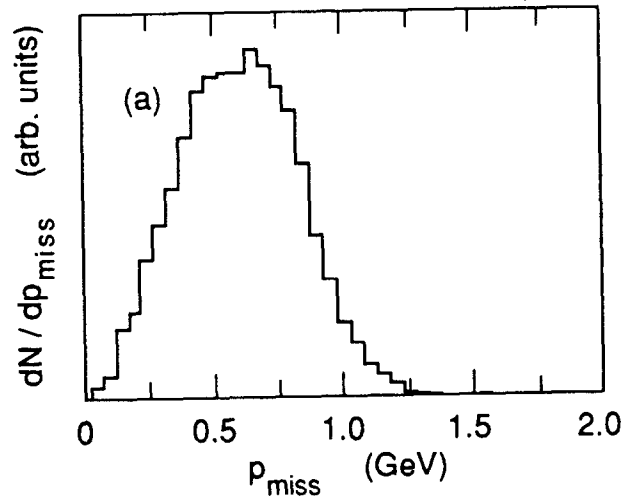


Fig. 6

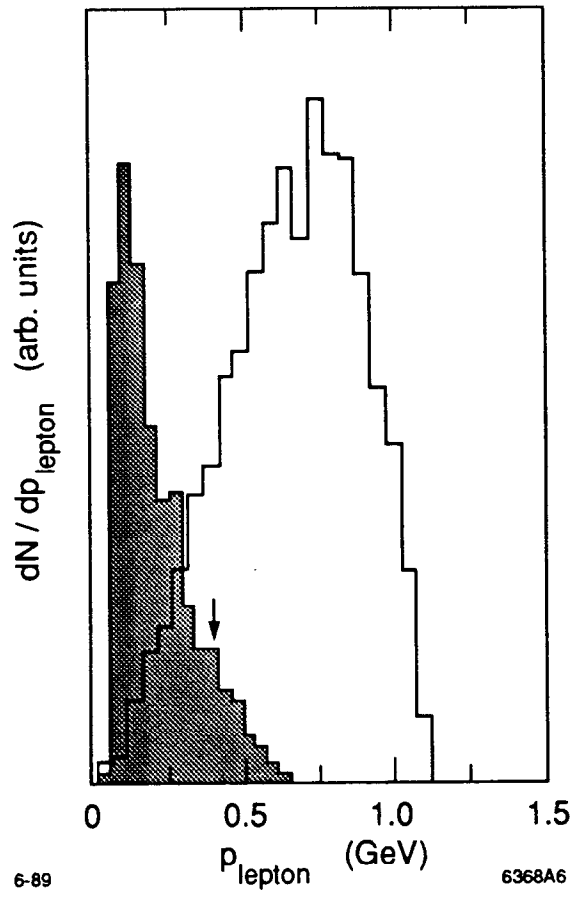


Fig. 7

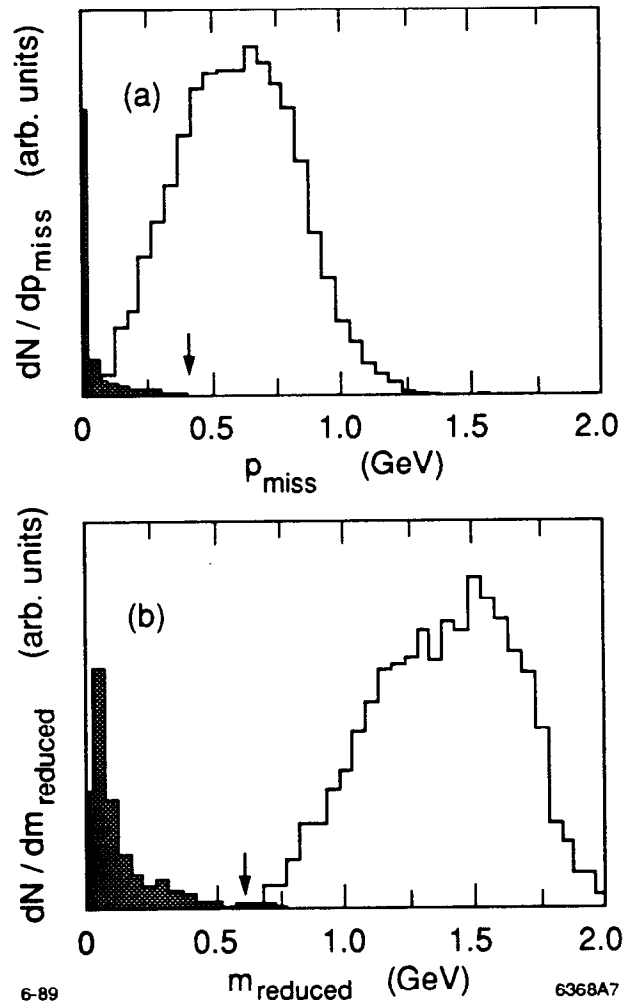


Fig. 8

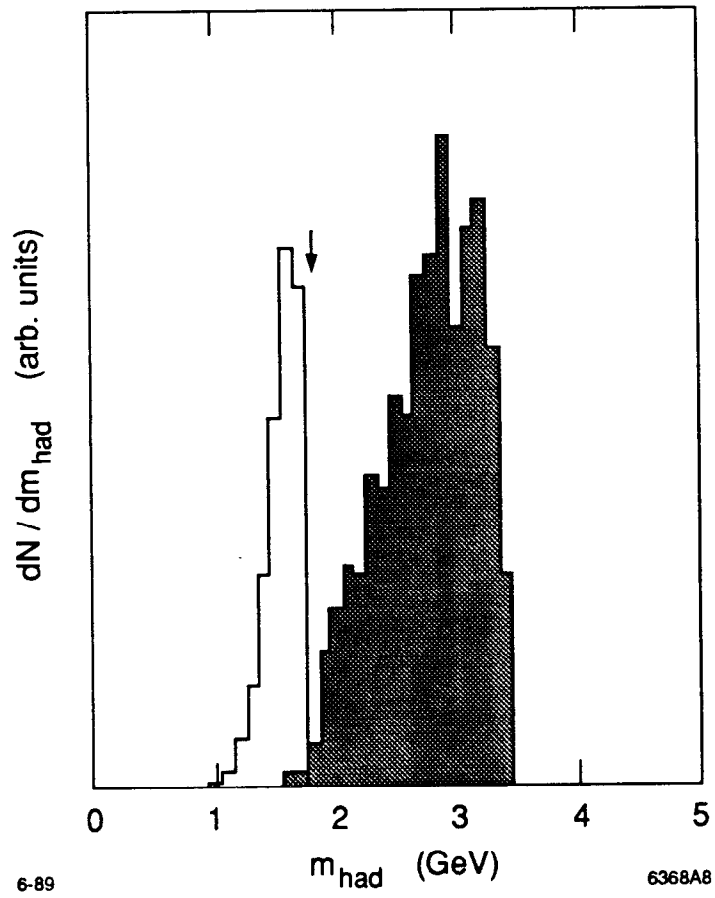
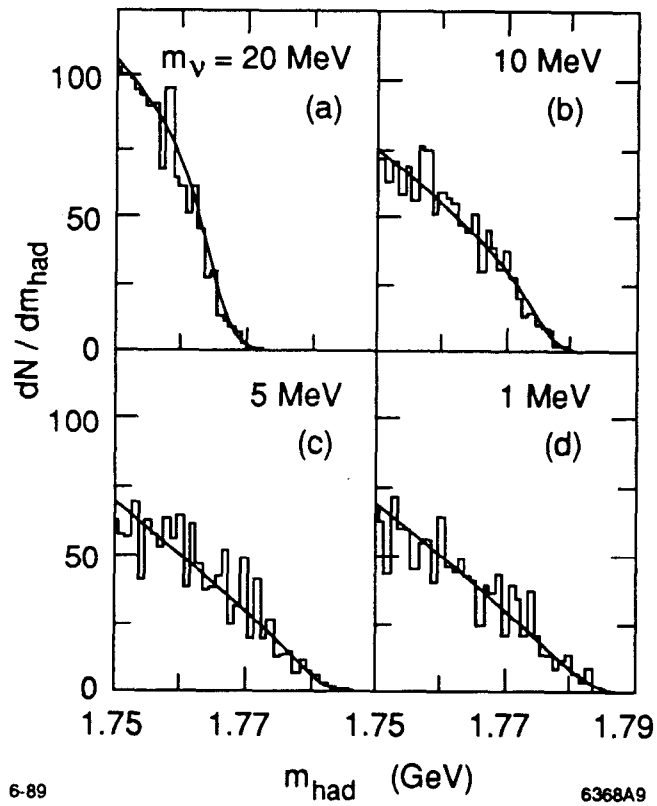


Fig. 9



6-89

6368A9

Fig. 10